NIH Public Access
Author Manuscript
AJR Am J Roentgenol. Author manuscript; available in PMC 2013 September 09.

Published in final edited form as:
AJR Am J Roentgenol. 2013 July ; 201(1): W57–W63. doi:10.2214/AJR.12.9579.

Primary Salivary Gland–Type Lung Cancer: Imaging and Clinical Predictors of Outcome

Amr ElNayal[1], **Cesar A. Moran**[2], **Patricia S. Fox**[3], **Osama Mawlawi**[4], **Stephen G. Swisher**[5], and **Edith M. Marom**[6]

[1]Department of Radiology, National Cancer Institute, Cairo, Egypt

[2]Department of Pathology, The University of Texas M. D. Anderson Cancer Center, Houston, TX

[3]Department of Biostatistics, The University of Texas M. D. Anderson Cancer Center, Houston, TX

[4]Department of Imaging Physics, The University of Texas M. D. Anderson Cancer Center, Houston, TX

[5]Department of Thoracic Surgery, The University of Texas M. D. Anderson Cancer Center, Houston, TX

[6]Department of Diagnostic Radiology, The University of Texas M. D. Anderson Cancer Center, 1515 Holcombe Blvd, Unit 1478, Houston, TX 77030

Abstract

OBJECTIVE—The objective of our study was to assess whether CT features and FDG uptake of primary salivary gland–type tumors of the lung are associated with tumor type, disease stage, or survival.

MATERIALS AND METHODS—CT ($n = 30$) and PET ($n = 15$) data of 30 consecutive patients with primary salivary gland–type tumors of the lung were retrospectively evaluated for tumor size, location, and homogeneity and the presence of lymphadenopathy, pleural effusions, and metastases. Maximum FDG uptake and volumetric FDG uptake of the tumors were recorded. The Wilcoxon rank sum and Fisher exact tests and univariate Cox regression were used for statistical calculations.

RESULTS—Compared with mucoepidermoid carcinomas, adenoid cystic carcinomas (57%) were larger (mean, 3.5 vs 2.2 cm, respectively; $p = 0.03$), more frequently involved the central airways (94% vs 63%; $p = 0.002$), and had a higher median FDG uptake ($p = 0.0264$). Higher FDG uptake of the primary tumor was associated with nodal tumor involvement ($p = 0.05$). The median overall survival times for patients with adenoid cystic carcinoma and mucoepidermoid carcinoma were 7.7 and 4.0 years, respectively. Imaging features that significantly affected overall survival included the presence of mediastinal or hilar lymphadenopathy (hazard ratio [HR], 4.33; 95% CI, 1.15–16.26; $p = 0.03$), suspected metastatic disease (HR, 5.10; 95% CI, 1.27– 20.47; $p = 0.02$), and primary tumor heterogeneity (HR, 3.46; 95% CI, 1.04–11.55; $p = 0.04$).

CONCLUSION—Higher FDG uptake is associated with nodal disease in patients with primary salivary gland–type tumors of the lung but is not predictive of survival, whereas CT features suggestive of advanced disease correlate with worse outcome.

© American Roentgen Ray Society

Address correspondence to: E. M. Marom (emarom@mdanderson.org).

NIH-PA Author Manuscript

NIH-PA Author Manuscript

NIH-PA Author Manuscript

NIH-PA Author Manuscript

NIH-PA Author Manuscript

NIH-PA Author Manuscript

Keywords

adenoid cystic carcinoma; CT; mucoepidermoid carcinoma; PET; salivary gland tumor

Primary salivary gland–type tumors of the lung occur primarily in the central airways and presumably originate from the submucosal glands. These tumors include adenoid cystic carcinomas (ACCs), mucoepidermoid carcinomas (MECs), and epithelial-myoepithelial carcinomas (EMECs) [1]. Most ACCs in the lung occur in the lower trachea or mainstem bronchi; a peripheral or segmental location is uncommon (10% of cases). Lung ACCs have a striking tendency toward submucosal extension within the airway [2, 3]. MECs are more commonly observed in segmental bronchi than in the trachea or main bronchi and appear as sharply marginated, either ovoid or lobulated, intraluminal nodules that adapt to the branching features of the airways [4]. A much less common entity that has been recognized only within the past 2 decades is primary pulmonary EMEC, which appears to be a low-grade malignant neoplasm with a low risk of recurrence after surgical excision [5, 6].

Primary salivary gland–type tumors of the lung differ from the more common types of lung cancer (adenocarcinoma and squamous cell carcinoma) in that the former tend to occur in younger patients [7–9], to affect the central airways, and to have a more indolent nature [10, 11]; however, staging and treatment of primary salivary gland–type tumors do not differ from the staging and treatment of adenocarcinoma or squamous cell carcinoma. Unlike staging of adenocarcinoma and squamous cell lung cancers, which are predominantly affected by positive nodal and metastatic disease, staging of primary salivary gland–type tumors of the lung is usually affected most by the primary local tumor invasion because they usually present without metastatic disease. Failure to identify tumor growth along the airways or in the submucosa leads to incorrect delineation and staging of primary salivary gland– type tumors of the lung, which impacts treatment planning—that is, surgical and radiation planning. Inadequate planning can affect patients negatively because local recurrence is likely if complete surgical resection is not achieved [11].

One way to improve treatment planning is to determine whether information already obtained on CT or PET can be used for better tumor delineation. The purpose of our study was to assess the morphologic appearance of primary salivary gland–type tumors of the lung at presentation, determine whether any CT features of these tumors are associated with staging and outcome, and assess the role of ^{18}F-FDG PET/CT in the staging and treatment of these tumors.

Materials and Methods

Patients

For this retrospective study, we reviewed the University of Texas M. D. Anderson Cancer Center's electronic pathology database to identify patients who had been diagnosed with primary salivary gland–type tumor of the lung (ACC, MEC, or EMEC) between January 1, 2001, and September 15, 2010. We then reviewed those patients' electronic medical records to extract imaging data and data on demographic characteristics, tumor histology, treatment, stage (American Joint Committee on Cancer criteria), and survival times. Of the 53 patients with primary salivary gland–type tumor of the lung, 23 were excluded because pretreatment CT images were not available. Thus, the final study group comprised 30 patients who had been treated for primary salivary gland–type tumor of the lung and had a pretreatment CT study available for review.

NIH-PA Author Manuscript NIH-PA Author Manuscript NIH-PA Author Manuscript

Our cancer center's institutional review board approved this study and granted us a waiver of the requirement for informed consent. In addition, our study complied with HIPAA regulations.

Imaging

Chest CT scans of the 30 study patients had been obtained using a variety of helical scanners and slice thicknesses: 1.3 mm in two patients, 2.5 mm in seven, 3.8 mm in six, 4 mm in one, 5 mm in eight, 7 mm in one, 7.5 mm in one, and 8 mm in four. Images had been reconstructed using lung and soft-tissue kernels. IV nonionic contrast medium (120–150 mL ioversol [Optiray 320, Covidien]) had been administered via an antecubital vein at a rate of 3.0–4.2 mL/s with a 12- to 20-second delay in 27 patients.

For this analysis, chest CT scans were reviewed by two chest radiologists, and differences were resolved by consensus. The CT findings recorded for each patient were the size of the primary tumor, homogeneity of the tumor, tumor shape (smooth, lobulated, or circumferential airway thickening), whether the tumor was well marginated, the largest-order airway with tumor involvement, whether tumor had infiltrated the surrounding fat, the percentage of tumor abutting an adjacent mediastinal vessel ($< 50\%$ or $\geq 50\%$), whether pleural effusion was present, whether mediastinal or hilar lymphadenopathy was present, whether infradiaphragmatic metastases were present, and whether pulmonary nodules were present.

FDG PET or FDG PET/CT had been performed in 15 patients before any chemotherapy or tumor resection. Of those scans, seven were performed at our institution using an integrated PET/CT system (Discovery ST, STe, or RX, GE Healthcare). Whole-body examinations were performed from the level of the vertex of the skull or the orbits through the upper thighs. All patients fasted for a minimum of 6 hours and had a blood glucose level of 80–120 mg/dL (4.4–6.6 mmol/L) before the IV administration of 15–20 mCi (555–740 MBq) of FDG. Unenhanced CT was used for attenuation correction and diagnosis and included the following parameters: 3.75-mm axial slice placement, 140 kV, 120 mA, and a 13.5-mm table speed. Emission PET was performed in the 2D mode 60–90 minutes after FDG administration at 3–5 minutes per bed station. Attenuation-corrected and non–attenuation-corrected datasets were reconstructed.

We reviewed all available whole-body PET ($n = 4$) and PET/CT ($n = 11$) scans. In addition to documenting the FDG uptake in the tumor using the maximum standardized uptake value (SUV_{max}) based on body weight (BW), which we refer to as "SUV_{maxBW}," we obtained SUV_{max} measurements based on lean body weight (LBW), which we refer to as "SUV_{maxLBW}," for the seven PET/CT studies performed in our institution. We calculated the volume of FDG-avid tumor as the volume of tumor (in cm^3) within 42% of the SUV_{maxBW} as well as the volume of tumor above SUV_{maxBW} thresholds of 2.5, 3.0, 3.5, and 4.0.

In addition to quantifying FDG uptake, we attempted to estimate tumor length from the PET images alone.

Statistical Analysis

For continuous variables, the Wilcoxon rank sum test was used to assess association with tumor type, with *p* values computed using the normal approximation. For categoric variables, the Fisher exact test was used to assess association with tumor type. Overall survival (OS) time was calculated from the date of the initial pathologic diagnosis to the date of death or last follow-up. Progression-free survival (PFS) time was calculated from the date of initial pathologic diagnosis to the date of recorded tumor progression, death, or stability at

NIH-PA Author Manuscript

last follow-up, whichever came first. Kaplan-Meier survival curves were used to estimate survival, and the log-rank test was used to assess differences between groups. Univariate Cox regression models were used to predict OS and PFS times using clinical and imaging features of interest. Multivariate Cox regression models could not be fit owing to the small number of events. All p values were two-sided. A p value of < 0.05 was considered significant. No adjustment for multiple comparisons was made. All statistical analyses were performed using statistics software (SAS, version 9.2, SAS Institute) for Microsoft Windows.

Results

Patients and Disease Characteristics

The 30 patients with primary salivary gland–type tumor of the lung included 17 women and 13 men with a median age of 45.5 years (range, 17–82 years old). Tumor histologic diagnoses were ACC in 17 patients, MEC in 11 patients, and EMEC in two patients. For statistical calculations, EMEC data were combined with MEC data. There were no statistically significant differences in age or sex between patients with ACC and those with MEC or EMEC. Sixteen patients presented with stage I disease, three with stage II disease, eight with stage III disease, and three with stage IV disease. All cases of stage III disease occurred in patients with ACCs. A comparison of early disease (stage I or II) with advanced disease (stage III or IV) suggested that patients with MEC or EMEC presented with early disease more frequently (11/13, 85%) than patients with ACC (8/17, 47%; $p = 0.0575$). Most patients had been treated with surgery (21/30, 70%) regardless of tumor histology ($p = 1.000$), but complete resection was significantly more likely in patients with MEC or EMEC ($p = 0.0075$).

Imaging

CT—On CT, maximum tumor size was 0.8–11.4 cm, with a median value of 2.7 cm. ACC tumors (median, 3.5 cm) tended to be larger than MEC and EMEC tumors (median, 2.2 cm; $p = 0.0264$). Central airway involvement (trachea or main bronchi) was more commonly seen in patients with ACC tumors (16/17, 94%) than in those with MEC or EMEC tumors (5/13, 38%). MEC and EMEC tumors tended to involve smaller airways— that is, the lobar, segmental, and subsegmental bronchi ($p = 0.0016$) (Figs. 1 and 2).

There were no statistically significant differences observed between patients with ACC and those with MEC or EMEC for the other CT features assessed (Table 1).

PET—Of the 15 patients who had undergone FDG PET, FDG PET/CT scans were available for 11 and FDG PET scans for the remaining four. The median SUV_{maxBW} of the primary tumor was 5.8 (range, 1.5–17.6). Of the seven patients for whom full PET/CT data were available, the median SUV_{maxLBW} of the primary tumor was 4.3 (range, 3–14.1), the median volume of tumor within 42% of the SUV_{maxBW} was 13.01 cm^3 (range, 2.5– 43.9 cm^3), and the median volumes of tumor above the SUV_{maxBW} thresholds of 2.5, 3.0, 3.5, and 4.0 were 11.44 cm^3 (range, 1.5– 74.62 cm^3), 4.99 cm^3 (range, 0–54.86 cm^3), 1.76 cm^3 (range, 0–42.25 cm^3), and 1.37 cm^3 (range, 0–32.27 cm^3), respectively.

Tumors with an ACC histologic diagnosis had higher FDG uptake (SUV_{maxBW}: median, 8.6; range, 3.7–17.6) than MEC and EMEC tumors (SUV_{maxBW}: median, 4.5; range, 1.5–6.3; $p = 0.0390$) (Figs. 2 and 3). Results usually approached significance for the seven patients in whom FDG uptake was measured by SUV_{maxLBW} and as volumetric SUV measurements (Table 2).

NIH-PA Author Manuscript NIH-PA Author Manuscript NIH-PA Author Manuscript

Of the 15 patients who had PET/CT studies, five had nodal metastatic disease, all with ACC histology, with a median SUV_{maxBW} of 10 (range, 4–17.6). The 10 patients without nodal metastatic disease had a significantly lower median SUV_{maxBW} of 5 (range, 2.1– 12.9; p = 0.0498) (Figs. 2 and 3).

Of the 21 patients treated with surgery, nine had FDG PET scans (eight with PET/ CT and one with PET alone) performed a median of 22 days (range, 1–38 days) before surgery; none of these nine had received neoadjuvant therapy. The maximum tumor lengths estimated from PET were similar to the tumor lengths measured in the resected specimens during pathologic examinations in three patients but differed by 5 mm or more in six (67%) patients. These same nine patients had undergone CT a median of 13 days before surgery (range, 1–38 days), and the maximum tumor lengths estimated from CT were similar to the tumor lengths measured in the resected specimens in five patients but differed by 5 mm or more in four (44%) patients. In two patients, the pathologic tumor specimens were 15 and 12 mm longer than estimated by PET and 9 and 3 mm longer than estimated by CT, respectively, even though each patient's imaging studies were performed on the same day.

Survival

The median OS and PFS times for all 30 patients were 7.7 years (n = 30, events = 11) and 7.8 years (n = 29, events = 13), respectively. The 3- and 5-year OS rates were 0.8475 and 0.6481 with standard errors of 0.0707 and 0.1026, respectively.

The only clinical variables analyzed that affected OS and PFS with $p < 0.05$ were treatment with surgery and stage (Figs. 4 and 5). Patients who were surgically treated had a significantly decreased risk of death (HR, 0.225; 95% CI, 0.060–0.846; p = 0.0273) and of disease progression (HR, 0.136; 95% CI, 0.031– 0.601; p = 0.0084) than patients treated with radiation, chemotherapy, or both but not surgery. Patients with stage III or IV disease had increased risk of death (HR, 4.686; 95% CI, 1.205–18.212; p = 0.0258) and progression (HR, 5.713; 95% CI, 1.602–20.375; p = 0.0072) than patients with stage I or II disease.

Regarding imaging variables, CT evidence of either hilar or mediastinal lymphadenopathy was associated with an increased risk of death (HR, 4.327; 95% CI, 1.151– 16.262; p = 0.0301) and of disease progression (HR, 4.903; 95% CI, 1.163–20.672; p = 0.0304). The identification of metastatic disease by CT was associated with an increased risk of death (HR, 5.102; 95% CI, 1.271–20.474; p = 0.0215) but not progression (p = 0.1408). Also, patients with heterogeneous tumors had increased risk of death (HR, 3.458; 95% CI, 1.035–11.547; p = 0.0438) but not progression (p = 0.2681). No other clinical or imaging variables analyzed including FDG uptake significantly affected OS or PFS times ($p > 0.05$).

Discussion

Our assessment of the morphologic features of primary salivary gland–type tumors of the lung on CT shows that CT features associated with shorter OS time were primary tumor heterogeneity, nodal enlargement, and imaging features suspicious for distant metastatic disease, whereas FDG uptake of the primary tumor was greater in ACC than in MEC and EMEC and was greater in cases with nodal involvement but was not significantly associated with survival time.

Primary salivary gland–type tumors of the lung are rare, accounting for fewer than 2% of all lung cancers. The most common histologic type is ACC, comprising about two thirds of the cases, whereas MEC comprises about a third and only a few EMEC primary salivary gland–type tumors of the lung have been described in the literature [11, 12]. The prognosis for patients with primary salivary gland–type tumor of the lung, with 5- and 10-year survival rates of 65% and 53%, respectively [11], is much better than the prognosis for patients with the more common lung cancers, such as adenocarcinoma (with a 5-year survival rate of 20%) and squamous cell carcinoma (with a 5-year survival rate of 17%) [10]. We were not able to confirm the worse OS time of patients with ACC compared patients with MEC that was shown in a larger study [11], probably because of our smaller sample size. Other evidence found in our study and in other studies [11, 13] points to the more aggressive nature of ACC, such as greater size of the primary tumor and the stronger association of ACCs with lymph node metastases and distant metastases. Our study, however, is the largest imaging study of primary salivary gland–type tumors of the lung to date. Although our results show that FDG uptake was much higher in ACC than in MEC and EMEC and was associated with nodal metastatic disease, increased FDG uptake did not translate into worse OS or PFS times. This lack of an association may be due to the statistical power given that only three of the 15 patients with SUV_{maxBW} measurements died. Thus, the lack of association of FDG uptake with survival could have been due not only to the sample size but also to the small number of deaths because the power for survival analyses is driven by the number of events (i.e., deaths, progressions). Our results need to be confirmed with a much larger imaging study.

In patients with primary salivary gland– type tumors of the lung, survival time after surgery is affected mainly by tumor stage [13]. Primary salivary gland–type tumors of the lung, particularly ACC and high-grade MEC, are infiltrative, and the amount of submucosal infiltration is often difficult to assess preoperatively and during surgery. Although single-detector CT scanners consistently underestimated the longitudinal extent of lesions [14], the introduction of MDCT with multiplanar reconstruction ability has improved the evaluation of the extent of tumors in airways [2, 3]. Because ACC is notorious for submucosal infiltration and, as shown in our study, is more likely to present with higher FDG uptake, it seems intuitive that one could better delineate the extent of tumor with FDG uptake and thereby improve preoperative estimation of tumor extent. The measurement of FDG uptake was even described in one case report [15] as a useful tool for the preservation of normal tissues by enabling treatment planning that minimized the irradiation of normal tissue. The accuracy of such FDG-based delineation was not verified in that report, which followed up the patient for 1 year; because the course of salivary gland tumors is variable and often indolent, the accuracy of a new imaging modality would have to be judged by pathologic confirmation or multiyear follow-up. Like in other indolent tumors, such as carcinoid tumors and well-differentiated adenocarcinomas [16, 17], FDG uptake in primary salivary gland–type tumors of the lung is variable. Although some tumors will have increased FDG uptake, some may be of lower grade; show low levels of FDG uptake [18, 19]; and, as seen in our study, have similar activity to the mediastinal background activity. Thus, the diagnosis and the determination of local tumor extent cannot rely on FDG uptake alone. In addition, because of the inherently low spatial resolution of PET scanners compared with CT scanners, small FDG-avid tumor deposits are difficult to detect and difficult to localize with precision. This pitfall of PET was seen in our study in which tumor extent measured on pathologic examination was more often closer to the size measured by CT than by FDG PET.

Despite the shortcoming of FDG PET/CT evaluation of primary tumor extent, our study showed that a higher SUV increased the likelihood of nodal metastatic disease. Our results imply that nodal sampling should be done before treatment planning when the SUV is high despite the indolent nature of primary salivary gland–type tumors of the lung because these tumors have a high likelihood of having a higher tumor stage than morphologic images alone might suggest and therefore may require a different treatment strategy, such as chemotherapy, instead of or in addition to radiation or surgery.

NIH-PA Author Manuscript NIH-PA Author Manuscript NIH-PA Author Manuscript

NIH-PA Author Manuscript

NIH-PA Author Manuscript

NIH-PA Author Manuscript

Our study's main limitation is its small size, despite being the largest imaging study of primary salivary gland–type tumors of the lung to date. The small number of cases is due to the fact that ours is a single-institution study of a very rare type of lung cancer. It is possible that larger multiinstitutional studies would find more useful associations between FDG uptake and survival that may affect management. However, it is doubtful that volumetric studies of these tumors will prove more useful than points of maximum FDG activity because so many of these tumors have large portions of uptake similar to the mediastinal background activity, making it difficult to differentiate normal tissues from abnormal tissues.

In conclusion, our study shows that the extent of primary salivary gland–type tumor of the lung is best delineated by CT and that the likelihood of ACC and nodal or distant metastatic disease is higher in primary salivary gland–type tumors of the lung with higher FDG uptake.

Acknowledgments

This work was supported in part by the National Cancer Institute (Office of Cancer Center Support Grant P30 CA016672).

References

1. Beasley MB, Brambilla E, Travis WD. The 2004 World Health Organization classification of lung tumors. Semin Roentgenol. 2005; 40:90–97. [PubMed: 15898407]
2. Kim TS, Lee KS, Han J, Kim EA, Yang PS, Im JG. Sialadenoid tumors of the respiratory tract: radiologic-pathologic correlation. AJR. 2001; 177:1145–1150. [PubMed: 11641190]
3. Kwak SH, Lee KS, Chung MJ, Jeong YJ, Kim GY, Kwon OJ. Adenoid cystic carcinoma of the airways: helical CT and histopathologic correlation. AJR. 2004; 183:277–281. [PubMed: 15269011]
4. Kim TS, Lee KS, Han J, et al. Mucoepidermoid carcinoma of the tracheobronchial tree: radiographic and CT findings in 12 patients. Radiology. 1999; 212:643–648. [PubMed: 10478226]
5. Doganay L, Bilgi S, Ozdil A, Yoruk Y, Altaner S, Kutlu K. Epithelial-myoepithelial carcinoma of the lung: a case report and review of the literature. Arch Pathol Lab Med. 2003; 127:e177–e180. [PubMed: 12683896]
6. Wilson RW, Moran CA. Epithelial-myoepithelial carcinoma of the lung: immunohistochemical and ultrastructural observations and review of the literature. Hum Pathol. 1997; 28:631–635. [PubMed: 9158714]
7. Heitmiller RF, Mathisen DJ, Ferry JA, Mark EJ, Grillo HC. Mucoepidermoid lung tumors. Ann Thorac Surg. 1989; 47:394–399. [PubMed: 2930303]
8. Moran CA, Suster S, Koss MN. Primary adenoid cystic carcinoma of the lung: a clinicopathologic and immunohistochemical study of 16 cases. Cancer. 1994; 73:1390–1397. [PubMed: 7509254]
9. Yousem SA, Hochholzer L. Mucoepidermoid tumors of the lung. Cancer. 1987; 60:1346–1352. [PubMed: 3040215]
10. Gloeckler Ries, LA.; Eisner, MP. Cancer of the lung. In: Ries, LAS.; Young, JL.; Keel, GE.; Eisner, MP.; Lin, YD.; Horner, M-J., editors. SEER survival monograph: cancer survival among adults—US SEER Program, 1988–2001, patient and tumor characteristics. Bethesda, MD: National Cancer Institute, SEER Program, NIH; 2007. p. 73-80.
11. Molina JR, Aubry MC, Lewis JE, et al. Primary salivary gland–type lung cancer: spectrum of clinical presentation, histopathologic and prognostic factors. Cancer. 2007; 110:2253–2259. [PubMed: 17918258]
12. Nguyen CV, Suster S, Moran CA. Pulmonary epithelial-myoepithelial carcinoma: a clinicopathologic and immunohistochemical study of 5 cases. Hum Pathol. 2009; 40:366–373. [PubMed: 18973918]
13. Kang DY, Yoon YS, Kim HK, et al. Primary salivary gland–type lung cancer: surgical outcomes. Lung Cancer. 2011; 72:250–254. [PubMed: 20884075]

NIH-PA Author Manuscript

NIH-PA Author Manuscript

NIH-PA Author Manuscript

14. Spizarny DL, Shepard JA, McLoud TC, Grillo HC, Dedrick CG. CT of adenoid cystic carcinoma of the trachea. AJR. 1986; 146:1129–1132. [PubMed: 3010684]
15. Haresh KP, Prabhakar R, Rath GK, Sharma DN, Julka PK, Subramani V. Adenoid cystic carcinoma of the trachea treated with PET-CT based intensity modulated radiotherapy. J Thorac Oncol. 2008; 3:793–795. [PubMed: 18594327]
16. Erasmus JJ, McAdams HP, Patz EF Jr, Coleman RE, Ahuja V, Goodman PC. Evaluation of primary pulmonary carcinoid tumors using FDG PET. AJR. 1998; 170:1369–1373. [PubMed: 9574618]
17. Marom EM, Sarvis S, Herndon JE 2nd, Patz EF Jr. T1 lung cancers: sensitivity of diagnosis with fluorodeoxyglucose PET. Radiology. 2002; 223:453–459. [PubMed: 11997552]
18. Ishizumi T, Tateishi U, Watanabe S, Maeda T, Arai Y. F-18 FDG PET/CT imaging of low-grade mucoepidermoid carcinoma of the bronchus. Ann Nucl Med. 2007; 21:299–302. [PubMed: 17634848]
19. Jeong SY, Lee KS, Han J, et al. Integrated PET/CT of salivary gland type carcinoma of the lung in 12 patients. AJR. 2007; 189:1407–1413. [PubMed: 18029878]

NIH-PA Author Manuscript

NIH-PA Author Manuscript

NIH-PA Author Manuscript

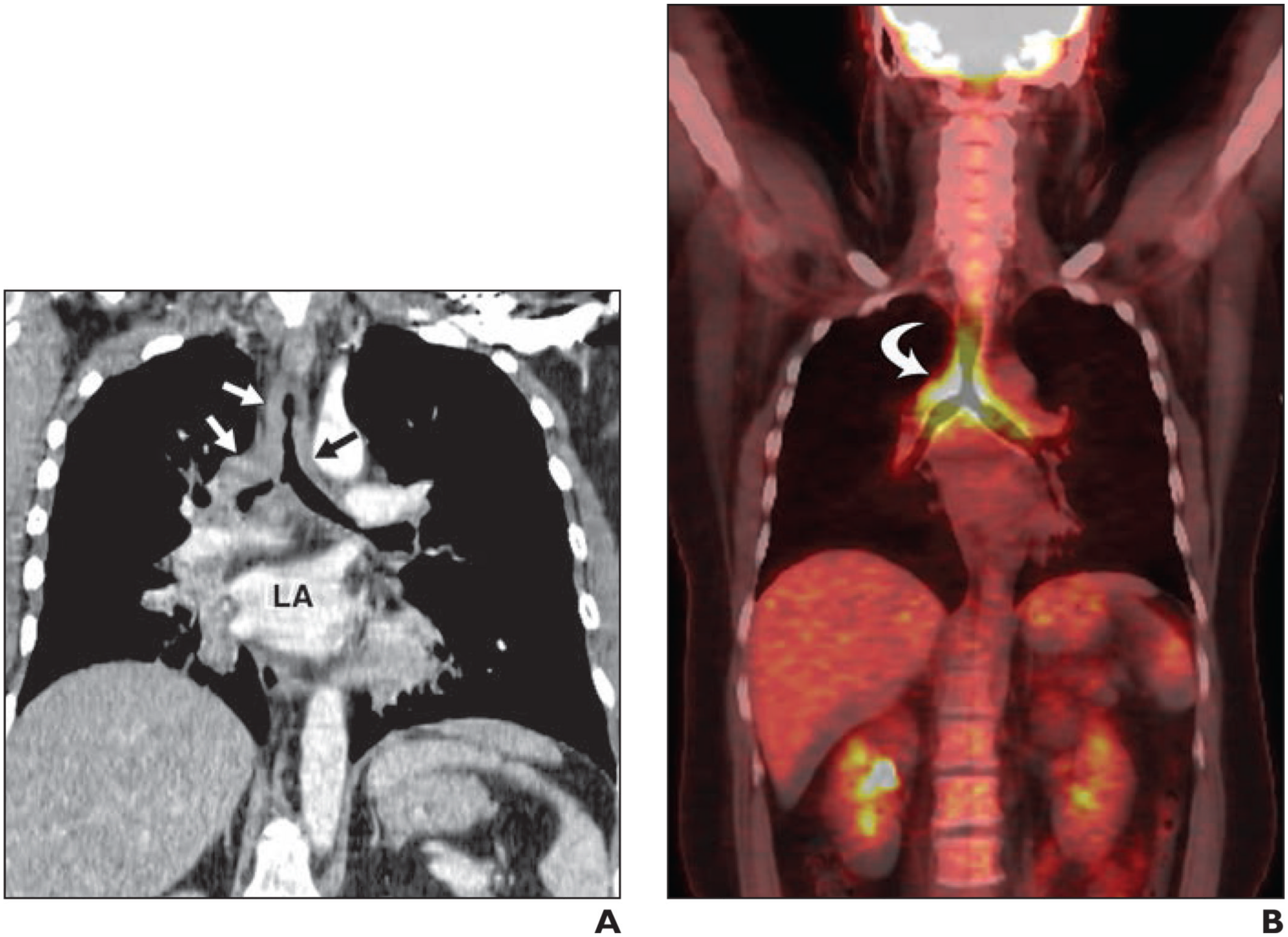

Fig. 1. 37-year-old woman with recurring respiratory infections

A, Coronal oblique reconstruction image of contrast-enhanced chest CT through left atrium (LA) shows circumferential airway thickening (*arrows*) involving trachea and main bronchi. **B**, FDG PET/CT image shows thickening (*arrow*) seen in **A** to have maximum standardized uptake value based on body weight of 8.6. Endobronchial biopsy from carina revealed adenoid cystic carcinoma.

NIH-PA Author Manuscript
NIH-PA Author Manuscript
NIH-PA Author Manuscript

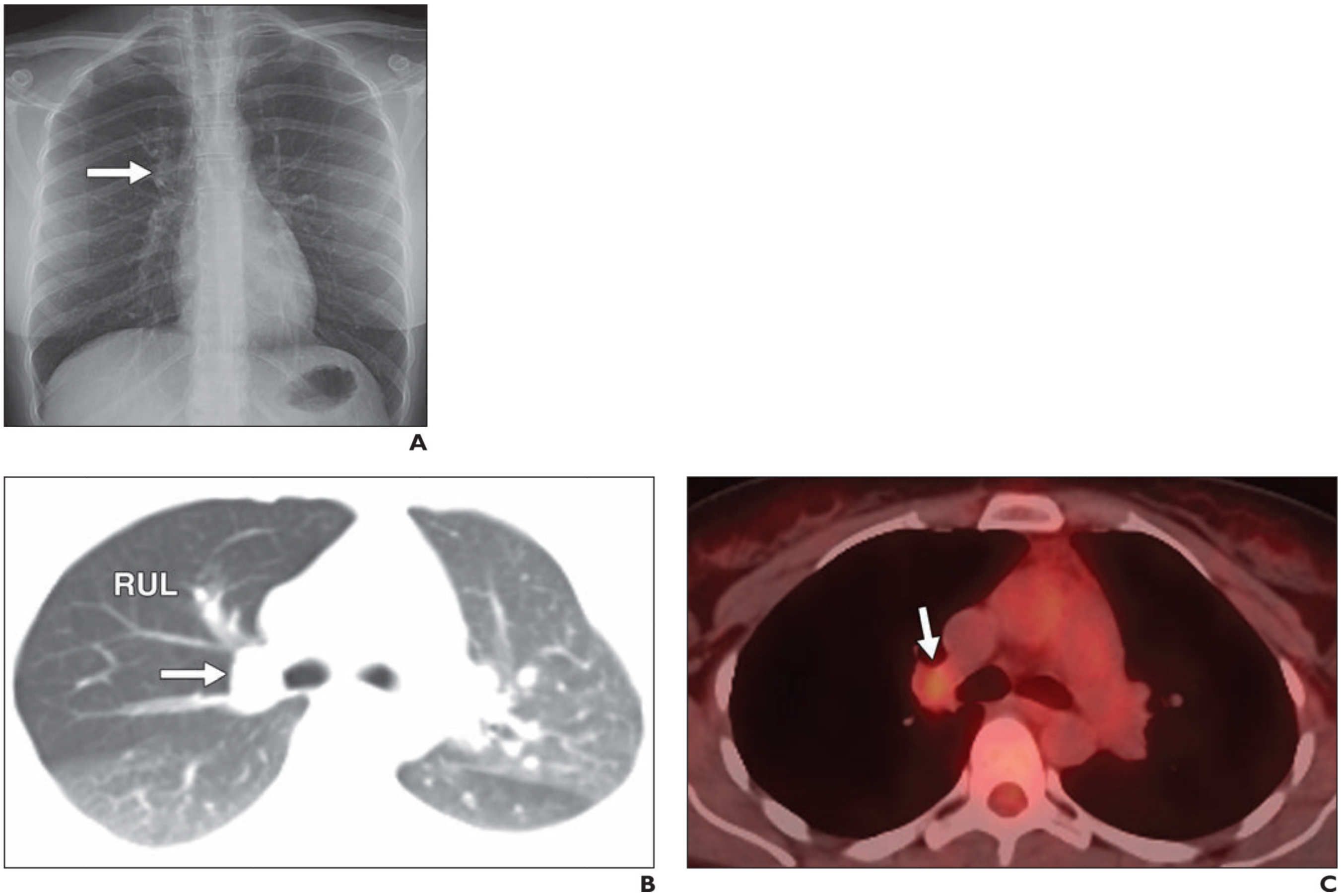

Fig. 2. 36-year-old woman with mucoepidermoid carcinoma

A, Frontal chest radiograph shows some fullness in right suprahilar region (*arrow*).

B, Axial oblique reconstructed contrast-enhanced chest CT image shows 2.2-cm nodule (*arrow*) in right upper lobe (RUL) obstructing right upper lobe bronchus and causing air trapping in right upper lobe.

C, PET/CT image corresponding to **B** shows only mild FDG uptake in nodule (*arrow*), with maximum standardized uptake value based on body weight of 2.1. At resection there was no nodal involvement.

NIH-PA Author Manuscript

NIH-PA Author Manuscript

NIH-PA Author Manuscript

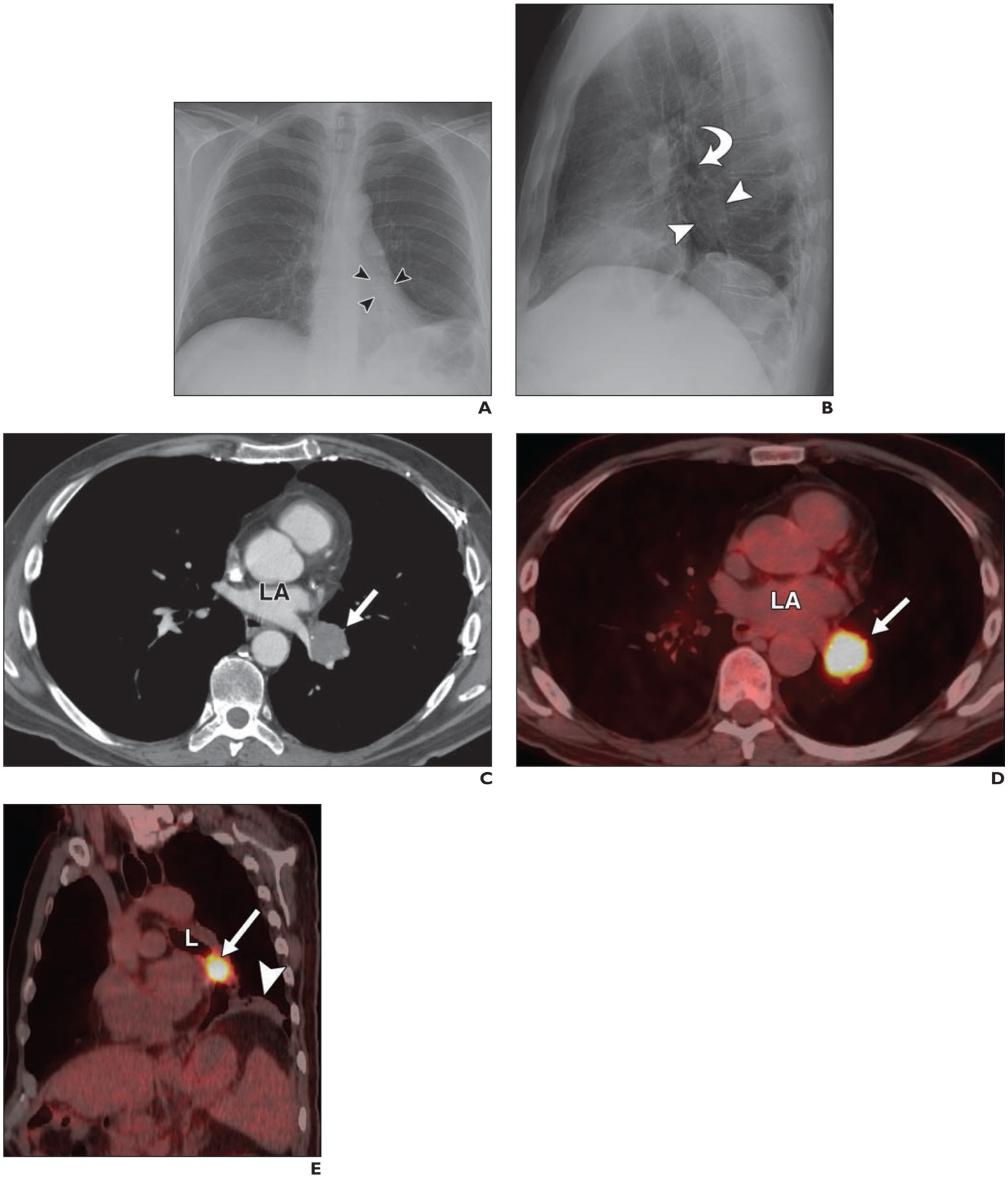

Fig. 3. 55-year-old man with adenoid cystic carcinoma of left lower lobe bronchus incidentally discovered on routine chest radiography

A and **B**, Posteroanterior (**A**) and lateral (**B**) chest radiographs show mass (*arrowheads*) below level of left upper lobe bronchus (*arrow*, **B**) with associated left lower lobe volume loss.

C, Contrast-enhanced chest CT image obtained at level of left atrium (LA) shows 3.7-cm mass (*arrow*) at level of left atrium.

D, Fused PET/CT image corresponding to **C** shows avid FDG uptake in mass (*arrow*) with maximum standardized uptake value based on body weight of 17.6. LA = left atrium.

NIH-PA Author Manuscript

NIH-PA Author Manuscript

NIH-PA Author Manuscript

E, Coronal oblique PET/CT image obtained through left lower lobe bronchus (L) shows mass (*arrow*) obstructing left lower bronchus and postobstructive pneumonitis (*arrowhead*). At resection of tumor, hilar lymph node showed metastatic disease.

NIH-PA Author Manuscript
NIH-PA Author Manuscript
NIH-PA Author Manuscript

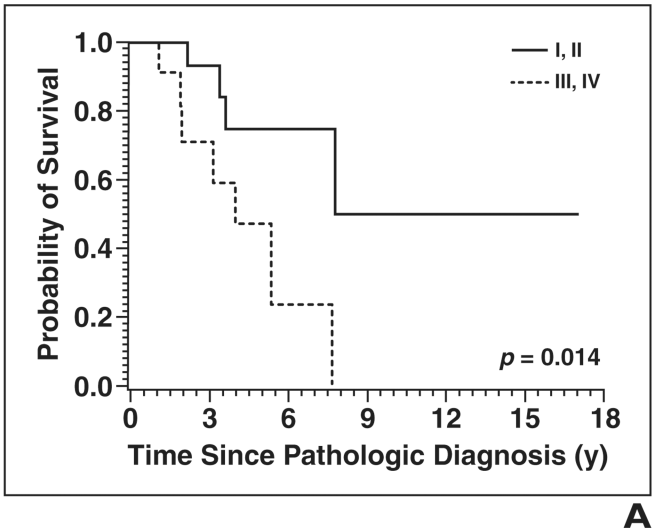

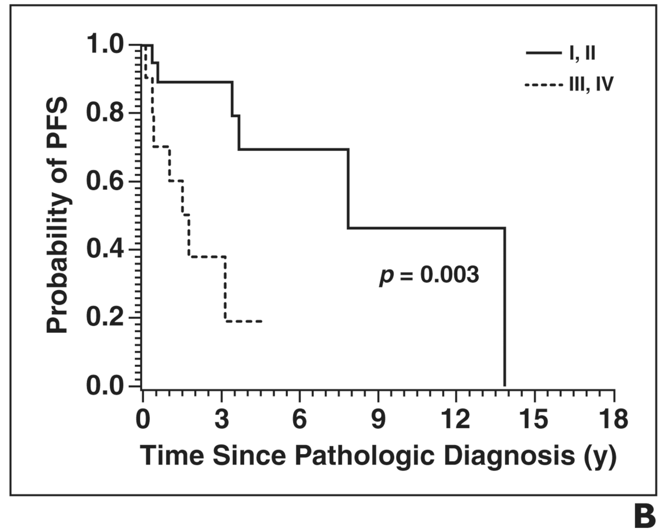

Fig. 4. Overall survival (OS) and progression-free survival (PFS) results by stage of disease

A and **B**, OS (**A**) and PFS (**B**) curves show patients with early disease, defined as stage I or II, had longer OS and PFS than those with advanced disease, defined as stage III or IV.

NIH-PA Author Manuscript

NIH-PA Author Manuscript

NIH-PA Author Manuscript

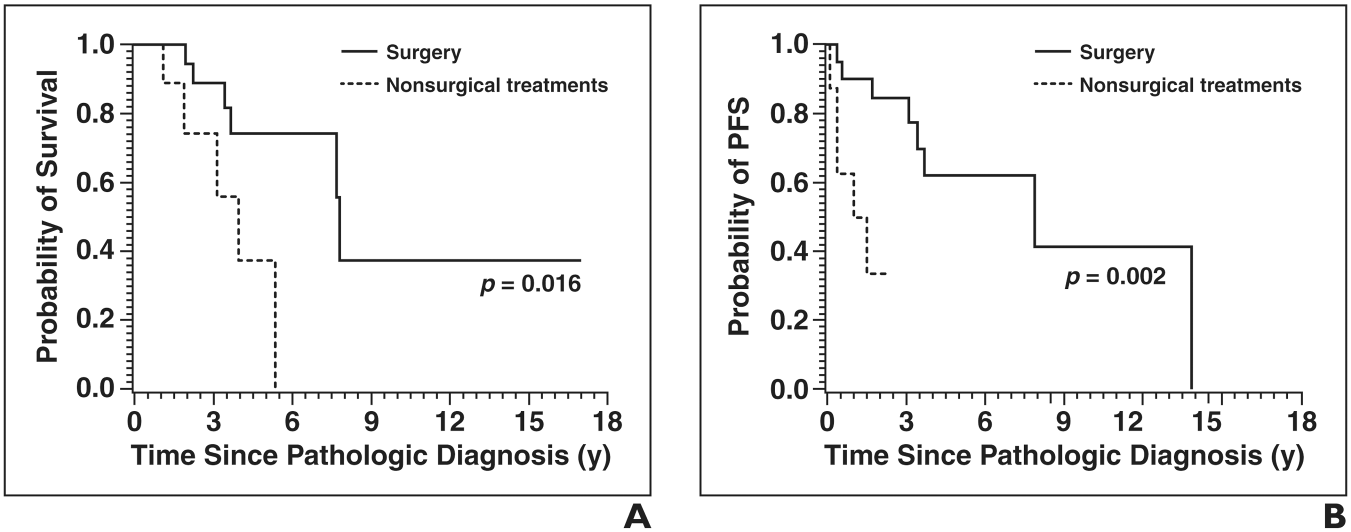

Fig. 5. Overall survival (OS) and progression-free survival (PFS) results by treatment

A and **B**, OS (**A**) and PFS (**B**) curves show patients treated with surgery had longer OS and PFS than those treated with chemotherapy, radiation therapy, or both.

NIH-PA Author Manuscript NIH-PA Author Manuscript NIH-PA Author Manuscript

TABLE 1

CT Findings by Type of Primary Salivary Gland–Type Lung Tumor

CT Feature	Tumor Type: ACC, No. of Patients	ACC, % of Patients	MEC and EMEC, No. of Patients	MEC and EMEC, % of Patients	Total No. of Patients	*p*
Homogeneous						0.6976
No	4	50	4	50	8	
Yes	13	59	9	41	22	
Shape						0.2100
Circumferential thickening	4	100	0	0	4	
Lobular	6	55	5	45	11	
Rounded	7	47	8	53	15	
Margin definition						1.0000
Poorly defined	3	50	3	50	6	
Well defined	14	58	10	42	24	
Largest-order airway with tumor extension[a]						0.0016
1, 2	16	76	5	24	21	
3, 4, 5	1	11	8	89	9	
Infiltration of surrounding fat						0.1961
No	12	50	12	50	24	
Yes	5	83	1	17	6	
Amount of tumor abutting adjacent mediastinal vessel						0.4621
<50%	7	47	8	53	15	
≥50%	10	67	5	33	15	
Pleural effusion						1.0000
No	15	56	12	44	27	
Yes	2	67	1	33	3	
Lymphadenopathy						0.6908
No	11	52	10	48	21	
Yes	6	67	3	33	9	

NIH-PA Author Manuscript NIH-PA Author Manuscript NIH-PA Author Manuscript

CT Feature	Tumor Type				Total No. of Patients	*p*
	ACC		MEC and EMEC			
	No. of Patients	% of Patients	No. of Patients	% of Patients		
Suspected metastases						0.6725
No	13	54	11	46	24	
Yes	4	67	2	33	6	

Note—Of these features, only central airway (trachea or main bronchi) involvement was more commonly associated with ACC than with MEC and EMEC. ACC = adenoid cystic carcinoma, MEC = mucoepidermoid carcinoma, EMEC = epithelial-myoepithelial carcinoma.

[a]Airway order: 1, trachea; 2, main bronchi; 3, lobar bronchi; 4, segmental bronchi; 5, subsegmental bronchi.

NIH-PA Author Manuscript

NIH-PA Author Manuscript

NIH-PA Author Manuscript

TABLE 2

FDG Uptake by Type of Primary Salivary Gland–Type Lung Tumor

	Tumor Type						
	ACC			MEC and EMEC			
Variable	**Median**	**Range**	**No. of Tumors**	**Median**	**Range**	**No. of Tumors**	***p***
SUV_{maxBW}	8.6	3.7–17.6	9	4.50	1.5–6.3	6	0.0390
SUV_{maxLBW}	9.8	5.3–14.1	3	3.75	3.0–4.3	4	0.0518
Volume of tumor (cm^3)							
Within 42% of the SUV_{maxBW}	23.6	4.4–43.9	3	9.61	2.5–24.4	4	0.5959
Above SUV_{maxBW} threshold of 2.5	41.4	14.6–74.6	3	3.56	1.5–11.1	4	0.0518
Above SUV_{maxBW} threshold of 3.0	35.4	11.7–54.9	3	1.74	0–5.0	4	0.0518
Above SUV_{maxBW} threshold of 3.5	30.0	9.5–42.3	3	0.78	0–1.8	4	0.0497
Above SUV_{maxBW} threshold of 4.0	25.0	8.1–32.3	3	0.00	0–1.4	4	0.0436

Note—ACC = adenoid cystic carcinoma, MEC = mucoepidermoid carcinoma, EMEC = epithelial-myoepithelial carcinoma, SUV_{maxBW} = maximum standardized uptake value based on body weight, SUV_{maxLBW} = maximum standardized uptake value based on lean body weight.